

SUPPLEMENTAL INFORMATION FOR "UNDERSTANDING THE SELF-ASSEMBLY OF CHAGED NANOPARTICLES AT THE WATER/OIL INTERFACE"

F. REINCKE, W.K. KEGEL, H. ZHANG, M. NOLTE, D. WANG, D. VANMAEKELBERGH,
H. MÖHWALD

ABSTRACT. This supplemental information describes a model which describes the adsorption of electrically charged, interfacially active nanocrystals at the water/heptane interface. Since dense systems of charged particles at the interface are inherently complex, this model is only intended as a first order approximation. First the chemical potential of particles in the bulk aqueous phase is calculated followed by the chemical potential of the particles at the interface. In the latter the particle surface coverage at the interface ϕ_s is required. Finally, using $\mu_{bulk} = \mu_{int}$ the equilibrium density of particles ϕ_s^{eq} can be derived.

1. THE CHEMICAL POTENTIAL FOR CHARGED NANOCRYSTAL IN THE AQUEOUS PHASE

We take the colloidal aqueous (bulk) phase to be sufficiently diluted so that interactions between the particles can be neglected. Also the particles are assumed to be monodisperse, equally charged and spherical, the latter condition results in translational degrees of freedom only. With these assumptions, there are two contributions to the bulk (Helmholtz) free energy. The first contribution is an "ideal gas"-like term which was found to be:¹

$$\frac{\mu_{ideal}}{kT} = \ln\left(\frac{\rho}{\rho^0}\right) \quad (1)$$

where ρ is the number density of particles in the aqueous bulk phase.

From a statistical analysis, it can be found that $\rho^0 = v_w^{-1}$, with v_w the water volume.¹

If a concentrated colloidal solution is used a term containing the second virial coefficient should be added. However, the size of the virial coefficient is negligible compared to the electrostatic repulsion of particles at the interface which will be discussed later.

The second contribution is the free energy of the particle-solvent interface, which is given by

$$F_{c/w} = 4\pi R^2 N \gamma_{c/w} \quad (2)$$

where N is the number of colloids, $\gamma_{c/w}$ is the interfacial tension between water (solvent) and the colloidal particle, and R the particle radius.

Combining the two contributions and using $\mu = \left(\frac{\partial F}{\partial N}\right)_{T,V}$ we obtain the chemical potential of a particle in the bulk water phase:

$$\frac{\mu_{bulk}}{kT} = \ln\left(\frac{v_w}{v_p}\right) + \ln(\phi) + \frac{4\pi R^2 \gamma_{c/w}}{kT} \quad (3)$$

In this equation, the particle volume $v_p = \frac{4}{3}\pi R^3$, and $\phi = v_p \rho$ is the volume fraction of the colloids in the water phase.

2. THE CHEMICAL POTENTIAL FOR CHARGED NANOCRYSTAL AT THE WATER/OIL INTERFACE

The chemical potential of a charged nanocrystal at the water/organic interface is determined by three types of interactions:

- a. The energy of the water/organic, water/particle and particle/organic interfaces in the system and the translational entropy of the particles at the interface;
- b. Electrostatic repulsions between the colloids adsorbed at the interface. We have investigated three different descriptions: the direct and screened Coulomb repulsions, and the dipole interactions between the incomplete double layer around the colloids;
- c. The attractive van der Waals interactions between colloidal particles adsorbed at the interface.

ad a. The Helmholtz free energy due to interfacial tension is calculated by adding the contributions for every interface, given by $F_\gamma = \sum_i A_i \gamma_i$ where A_i and γ_i are the area and interfacial tension of interface i respectively. The interfacial properties depend strongly on the positioning of colloids at the interface. In most experiments nanocrystals are used with a three-phase contact angle very close to 90° .^{2,3} Moreover, Aveyard *et al.* showed that nanocrystals with $R < 20 \text{ nm}$ are only interfacially active when $\theta \approx 90^\circ$.⁴ Therefore we will take the particles to be halfway in the interface. Hence the interfacial energy is:

$$F_\gamma = (A - \pi R^2 N) \gamma_{o/w} + 2\pi R^2 N \gamma_{c/o} + 2\pi R^2 N \gamma_{c/w} + 2\pi R N \gamma_l \quad (4)$$

with $\gamma_{o/w}$, $\gamma_{c/o}$ and $\gamma_{c/w}$ are the interfacial tensions of the aqueous/organic, colloid/organic and colloid/aqueous interfaces, respectively, and γ_l is the line tension.

Using $\mu = \left(\frac{\partial F}{\partial N}\right)_{T,V}$ and the Young-Dupré equation $\gamma_{o/w} \cos \theta = \gamma_{c/o} - \gamma_{c/w}$ with $\theta = 90^\circ$, equation (4) results in

$$\mu_\gamma = -\pi R^2 \gamma_{o/w} + 4\pi R^2 \gamma_{c/w} + 2\pi R \gamma_l \quad (5)$$

Translational entropy of dense systems is extremely difficult to estimate, see, *e.g.*, Hoover *et al.*⁵ Dynamic light scattering experiments on both the colloidal solution and interfacial layer showed that the mobility is several orders of magnitude slower than in the bulk. This suggests that the particles in the interfacial layer of colloids are nearly completely immobilized and only the layers as a whole are free to move. Therefore, we choose to neglect the translational entropy altogether.

ad b. Since the particles at the interface are charged, repulsive electrostatic interactions occur between the charged particles at the interface. There has been debate about the nature of these electrostatic repulsions, which counteracts the decrease in interfacial energy. The aqueous and organic phase respond differently to the particle charge. The electric field propagates further through the organic phase than the aqueous phase due to the different dielectric constants (2-10 for organic solvents, versus 78 for water). Moreover, the surface charge is screened by ions dissolved in the aqueous phase. This has led to various descriptions of the pair repulsion energy V .

Firstly, there is the unscreened Coulomb interaction which is most likely to take place through the organic phase:⁴

$$V_{Unscreened} = \frac{\left(\frac{1}{2} A \alpha \sigma\right)^2}{4\pi \varepsilon_{organic} \varepsilon_0 r} \quad (6)$$

with A the particle surface area, σ the measured surface charge density, r the center to center distance of the particles, ε and ε_0 the relative dielectric constant and the permittivity

of vacuum respectively. It is likely that some of the surface charge, due to charged species adsorbed at the colloid interface, is transferred to the water phase. Also some of the charged species could recombine with their counter-ion. However, some charge residue can still be present at the organic/colloid interface. Therefore the factor α is used in equation (6).

Secondly, there is the screened Coulomb through the aqueous phase. We use a Yukawa-style potential to model this interaction

$$V_{Screened} = \frac{\left(\frac{1}{2}A\sigma\right)^2}{4\pi\epsilon_{water}\epsilon_0} \frac{e^{-\frac{r}{L_D}}}{r} \quad (7)$$

Finally, since the double layer around the particle is removed at the oil-side, the dipole moment of the double layer at the water side is no longer compensated and therefore the particle exhibits a permanent dipole moment.^{6,7} Such particle dipoles interact, according to

$$V_{Dipole} = \frac{2(A\sigma L_D)^2}{4\pi\epsilon_{dipole}\epsilon_0 r^3} \quad (8)$$

Since the dipole interaction partially takes place through the organic phase, ϵ_{dipole} is likely to be a weighted average of the dielectric constant of the aqueous and organic phase.

The electrostatic free energy of the system in principle follows from a Boltzmann weighted sum over the electrostatic energies of all particle configurations. However, due to the long-range nature of the electrostatic interactions it is, in general, prohibitively difficult to calculate the total electrostatic energy. We will therefore make some drastic simplifications resulting in an analytic expression for the electrostatic free energy. This allows one to estimate the influence of electrostatic interactions on the adsorption density, at least in a qualitative way. We assume that the particles form a dilute two-dimensional hexagonal crystal at the water/organic interface. From geometric considerations it follows that the surface fraction $\phi_s = N\pi R^2/A$ can be calculated from $r = 2R\sqrt{\phi_s^*/\phi_s}$ with $\phi_s^* \equiv \phi_s(r = 2R) = \frac{1}{6}\sqrt{3}\pi$ the surface fraction of a hexagonal close-packed monolayer. For simplicity, we will assume that repulsion energies are pairwise additive. In that case, the electrostatic free energy may be written as $F_{el} \approx \frac{1}{2}zNV(r)$ with z the number of nearest neighbours. Again using $\mu = \left(\frac{\partial F}{\partial N}\right)_{T,V}$ the chemical potential contributions for the various electrostatic interactions reads

$$\mu_{Unscreened} = \frac{3z\pi R^3\alpha^2\sigma^2\sqrt{y}}{8\epsilon_{organic}\epsilon_0} \quad (9)$$

$$\mu_{Screened} = \frac{z\pi R^3\sigma^2}{8\epsilon_{water}\epsilon_0} \left(3\sqrt{y} + \frac{2R}{L_D}\right) e^{-\frac{2R}{L_D\sqrt{y}}} \quad (10)$$

$$\mu_{Dipole} = \frac{5z\pi R\sigma^2 L_D^2 y^{\frac{2}{3}}}{16\epsilon_{dipole}\epsilon_0} \quad (11)$$

where $y = \phi_s/\phi_s^*$.

ad c. While van der Waals interactions decay as the inverse distance to the power six for atoms, in the case of colloids this decay is much slower,⁸ *i.e.*,

$$V_{vdWaals} = -\frac{H}{12} \left(\frac{y}{1-y} + y + 2\ln(1-y) \right) \quad (12)$$

where H is the Hamaker constant.

The above result predicts a x^{-2} dependence which is correct for particles that are relatively close. Using the same simplifications as in deriving the electrostatic free energy we

get

$$\mu_{vdWaals} = -\frac{zH}{12} \left(\frac{y^2}{2(1-y)^2} + y + \ln(1-y) \right) \quad (13)$$

Adding all the interfacial contributions (equations (5) and (13)) we obtain the chemical potential of a particle adsorbed at the oil-water interface

$$\frac{\mu_{int}}{kT} = \mu_{electrostatic} + \frac{\pi R^2}{kT} \left(\frac{2\gamma_l}{R} - \gamma_{o/w} + 4\gamma_{c/w} \right) - \frac{zH}{12} \left(\frac{y^2}{2(1-y)^2} + y + \ln(1-y) \right) \quad (14)$$

where $\mu_{electrostatic}$ contains one or more of the electrostatic repulsion terms $\mu_{Unscreened}$, $\mu_{Screened}$ and μ_{Dipole} , equations (9) through (11), respectively. We will later discuss which term(s) are expected to be dominant.

3. COMBINING BULK AND SURFACE CONTRIBUTIONS

Setting $\mu_{bulk} = \mu_{int}$ leads to the interfacial density as a function of bulk density, charge density, Hamaker constant, particle size and interfacial tensions. By combining equations (3) and (14) we see that the contributions containing $\gamma_{c/w}$ cancel. Thus, the equilibrium surface fraction ϕ_s^{eq} follows by numerically solving

$$\frac{\pi R^2}{kT} \left(\frac{2\gamma_l}{R} - \gamma_{o/w} \right) - \frac{zH}{12} \left(\frac{y^2}{2(1-y)^2} + y + \ln(1-y) \right) + \mu_{electrostatic} = \ln \left(\frac{v_w}{v_p} \right) + \ln(\phi) \quad (15)$$

In fact, ϕ and ϕ_s are equilibrium fractions and are related to the initial volume fraction (*i.e.* before interfacial adsorption takes place) in the water phase, ϕ_{init} , by matter conservation:

$$\phi_{init} = \phi + \frac{4AR}{3V} \phi_s \quad (16)$$

with V the volume of the aqueous phase, as before. In our case $\frac{AR}{V}$ is always very small compared to ϕ_{init} so that in our calculations we set $\phi = \phi_{init}$.

4. DEPENDENCE OF μ_{bulk} AND μ_{int} WITH THE SURFACE COVERAGE ϕ_s

In figure 1, curve a, the bulk chemical potential μ_{bulk} is shown as a function of surface coverage for the case of gold nanocrystals ($R = 8 \text{ nm}$) at the water/heptane interface after addition of ethanol. Since we have set $\phi = \phi_{init}$, μ_{bulk} is independent of the surface fraction ϕ . The value of μ_{bulk} is typically in the order of several tens of kT and is positive or negative depending mainly on the bulk concentration and $\gamma_{c/w}$. The dependence of the interfacial chemical potential (figure 1, curve b) on the particle surface density is more pronounced. To explain this behaviour we will discuss the interfacial density dependence of the different terms of μ_{int} . The interfacial energy term (figure 1, curve c) is independent of the surface coverage and has a value in the order of -100 kT . This term is much more important than the bulk chemical potential; the bulk properties will thus only have a minor effect on the surface coverage. The electrostatic repulsion terms (figure 1, curves d through f) are all 0 at $\phi_s = 0$ and increases to a finite positive value at $\phi_s = \phi_s^*$. It can be seen in figure 1, curve e, that $\mu_{screened}$ is at most on the order of several kT , whereas the other electrostatic interactions easily are on the order of several tens of kT . This

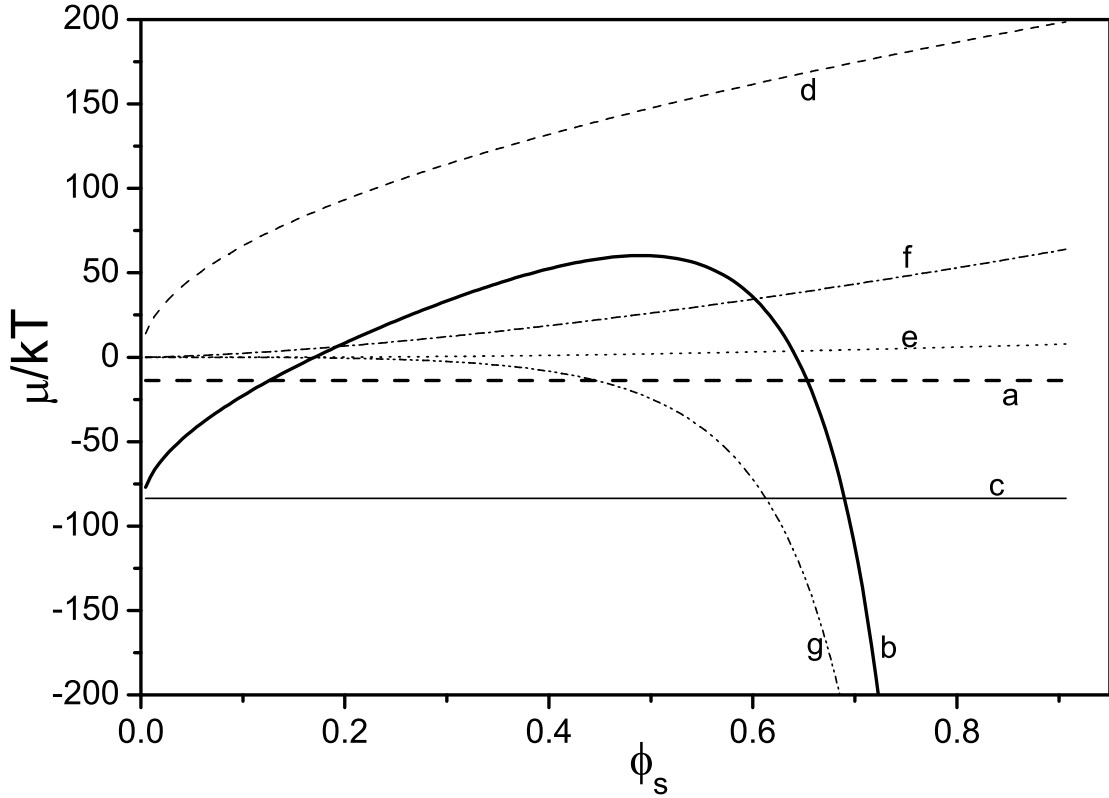


FIGURE 1. Results of the model calculations for typical values of the colloidal solution/heptane system. The chemical potential of particles in the aqueous bulk phase (curve a and equation (3)) and at the water/heptane interface (curve b and equation (14)). Curves c through g are the different contributions for the interfacial chemical potential, *viz.* interfacial energy (curve c and equation (4)), unscreened Coulomb repulsion through the organic phase (curve d and equation (9)), screened Coulomb repulsion through the water phase (curve e and equation (10)), dipole repulsion due to incomplete double layers around the particles (curve f and equation (11)), and van der Waals attraction (curve g and equation (13)). Values used were $R = 8 \text{ nm}$, $\sigma = 0.01 \text{ C/m}$, $z = 6$, $L_D = 4.5 \text{ nm}$, $\gamma_{c/w} \ll \gamma_{o/w}$, $\gamma_l = 0 \text{ N}$, $\alpha = 0.2$, $T = 298 \text{ K}$, $\epsilon_{\text{organic}} = 2$, $\epsilon_{\text{water}} = 80$, and $\epsilon_{\text{dipole}} = 41$. The surface tension of the water/heptane interface (50 mN/m) was measured using a Wilhelmy plate; this value was used for $\gamma_{o/w}$. The surface charge density σ followed from electrophoretic measurements.² L_D was calculated with the well-known Debye formula. Since the particle is half-way in the interface, the dipole interaction was assumed to equally interact through the water and heptane interface, therefore ϵ_{dipole} was set to 41.

is due to the fact that the screened Coulomb interaction occurs through the water phase whereas the dipole interaction occurs, partially, through the organic phase ($\epsilon_{\text{water}} = 80$, and $\epsilon_{\text{dipole}} = 41$). Even when curve e of figure 1 is not corrected for the dielectric constant the effect of screened Coulomb interactions is negligible with respect to the other electrostatic interactions and will therefore be neglected. The van der Waals term is also 0 at $\phi_s = 0$, but decreases to minus infinity at $\phi_s = \phi_s^*$.

Assuming that both dipole and unscreened Coulomb interactions are present, the interfacial chemical potential μ_{int} is calculated by adding the contributions for the interfacial

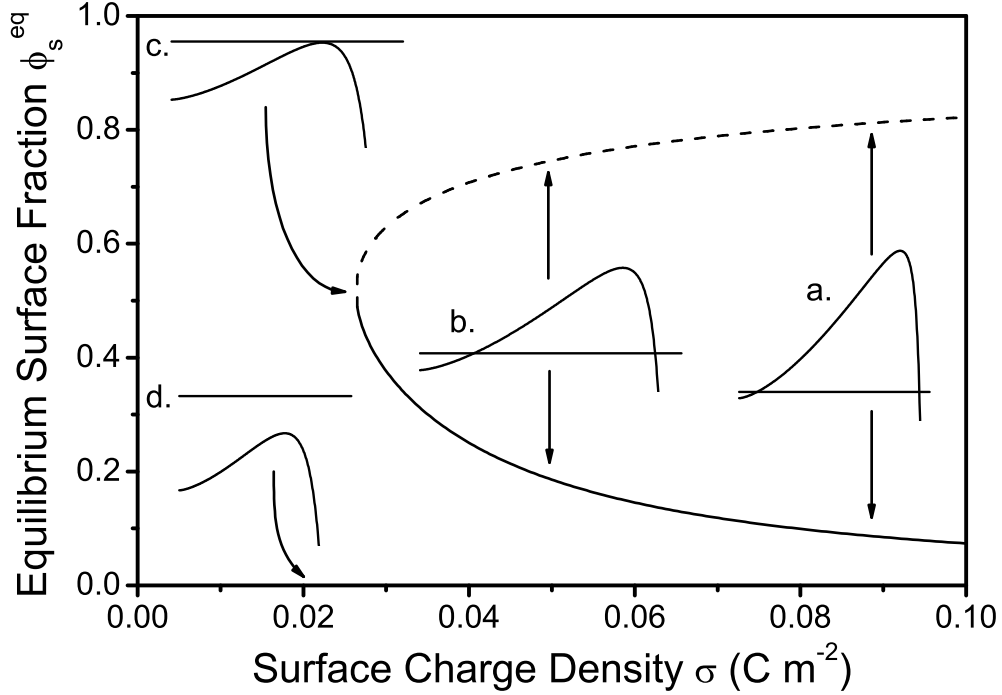


FIGURE 2. Results of the model calculations for typical values of the colloidal solution/heptane system. The equilibrium surface fraction ϕ_s^{eq} is plotted against particle surface charge density σ as calculated with equation (15). For reference, insets a. through d. show the approximate shape of μ_{bulk} (equation (3)) and μ_{int} (equation (14)) at the specific surface charge density. Values used were $R = 8 \text{ nm}$, $\sigma = 0.01 \text{ C/m}$, $z = 6$, $L_D = 4.5 \text{ nm}$, $\gamma_{c/w} \ll \gamma_{o/w}$, $\gamma_l = 0 \text{ N}$, $\alpha = 0.2$, $T = 298 \text{ K}$, $\epsilon_{organic} = 2$, $\epsilon_{water} = 80$, and $\epsilon_{dipole} = 41$. The surface tension of the water/heptane interface (50 mN/m) was measured using a Wilhelmy plate; this value was used for $\gamma_{o/w}$. The surface charge density σ followed from electrophoretic measurements.² L_D was calculated with the well-known Debye formula. Since the particle is half-way in the interface, the dipole interaction was assumed to equally interact through the water and heptane interface, therefore ϵ_{dipole} was set to 41.

energy, the Coulomb, dipole, and the van der Waals terms (figure 1, curves c, d, f, and g, respectively). This result is shown in curve b of figure 1. At small surface coverage (small ϕ_s) the interfacial energy term dominates the interfacial chemical potential. Going to $\phi_s \approx 0.4$ the electrostatic repulsion terms dominates and a maximum is reached. From $\phi_s \approx 0.6$, the van der Waals attraction becomes important and this drives the interfacial chemical potential to minus infinity at $\phi_s = \phi_s^*$. The height of the maximum of the chemical potential μ_{int} is determined by the value of $\mu_{electrostatic}$, which in itself is determined by the factor σ^2/ϵ , see equation (9) through (11).

5. EQUILIBRIUM SURFACE COVERAGE ϕ_s^{eq} VERSUS CHARGE DENSITY σ

In figure 2, **all** the calculated equilibrium surface fractions ϕ_s^{eq} are plotted as a function of the surface charge density σ . The insets of figure 2 show the shape of μ_{bulk} and μ_{int} at the indicated values of σ . At high surface charge density, see inset a. of figure 2, the model

predicts that two equilibrium surface densities; one at low surface density (solid line) and one at high surface charge density (dashed line). There are several arguments that the equilibrium at high surface charge density is an unphysical artifact in our model:

- The description of the van der Waals attraction has incorrect behavior when the colloids are in close proximity. Specifically, equation (13) goes to minus infinity at when $\phi_s = \phi_s^*$ ($\lim_{\phi_s \rightarrow \phi_s^*} \mu_{vdWaals} = -\infty$)
- Below a certain surface charge density, marked by inset c. in figure 2, the isotherm no longer has any solutions. This cannot be correct.

Therefore the complete high density branch (dashed line in figure 2) is ignored in the main paper.

If the surface charge density is lowered, see inset b. of figure 2, the electrostatic repulsion between the particles at the interface decrease. As a result, the low density equilibrium (solid line) shifts to higher surface fraction. When σ is lowered ever further, i.e. going from inset c. to inset d. of figure 2, equation (15) no longer has any physically relevant solutions. Since at this surface charge $\mu_{int} < \mu_{bulk}$ it is expected that all particles adsorb at the liquid/liquid interface.

6. SUPPLEMENTAL FIGURES

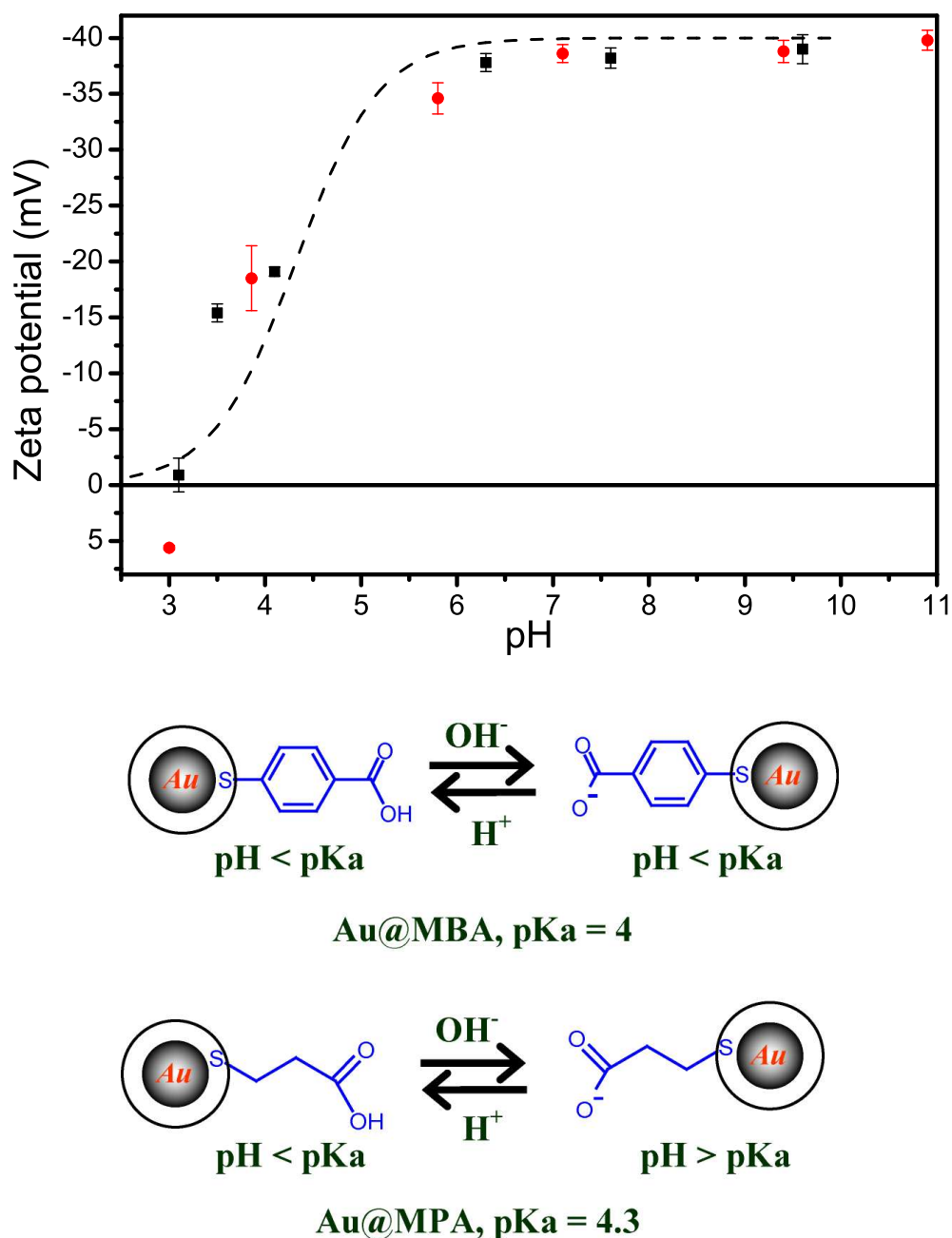


FIGURE S1. (Upper panel) Plot of zeta-potentials of Au nanocrystals with mean size of 6 nm, capped with 3-MPA (black square) and 4-MBA (red circle), versus pH. The dashed line is the calculated titration curve of 3-MPA (pKa of 4.32). (Lower panel) A schematic illustration of protonation and de-protonation of the Au nanocrystals.

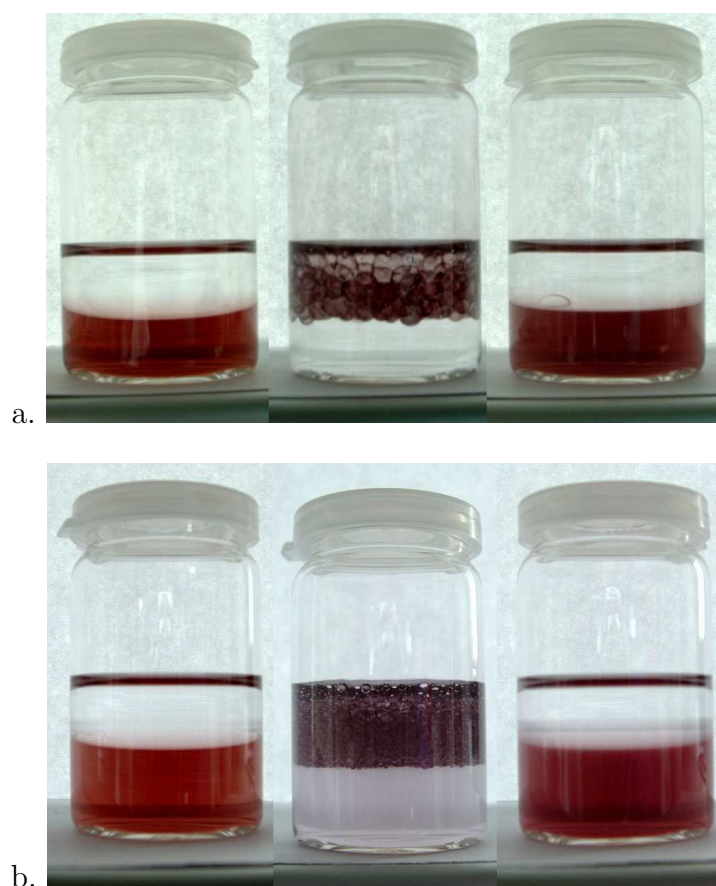


FIGURE S2. Photographs of glass vials containing aqueous solutions (bottom) of Au nanocrystals with a mean size of 6 nm, capped with 4-MBA (a) and 3-MPA (b), in contact with heptane (top), in which the pH of the aqueous solution of the nanocrystals in the glass vials are approximately at 9 (left), 2 (middle) and 9 (right). The images were taken directly after shaking.

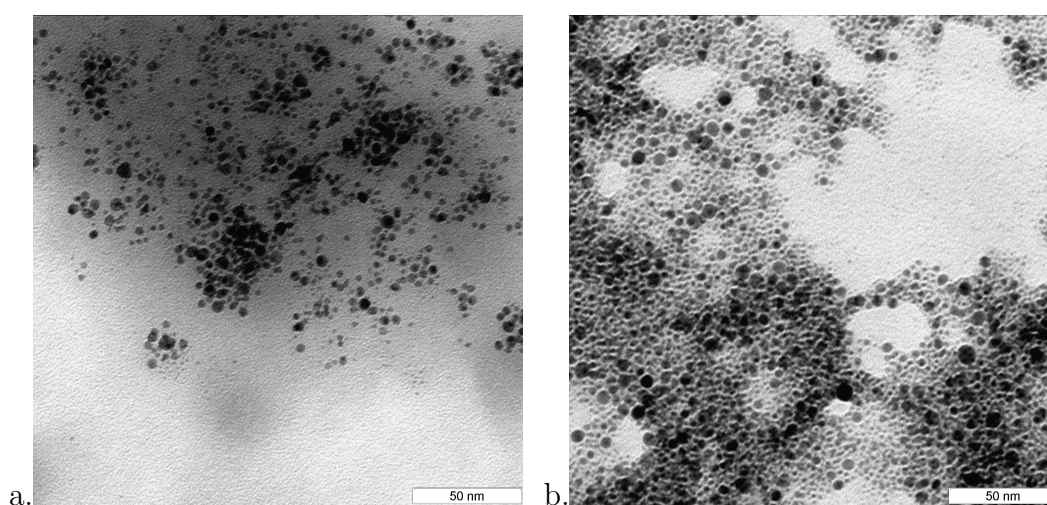


FIGURE S3. TEM images of 4-MBA-capped Au nanocrystals with mean size of 6 nm in the original solution (a) and self-assembled at the water/heptane interface (b).



FIGURE S4. Photographs of glass vials containing aqueous solutions (bottom) of 4-MBA-capped Au nanocrystals with a mean size of 6 nm in contact with heptane (top), after implementation of pH-switched self-assembly of the nanocrystals at the water/heptane interface 4 times. In the left glass vial, the pH of the aqueous solution of the nanocrystals was 9, while in the right vial, the pH was 2.

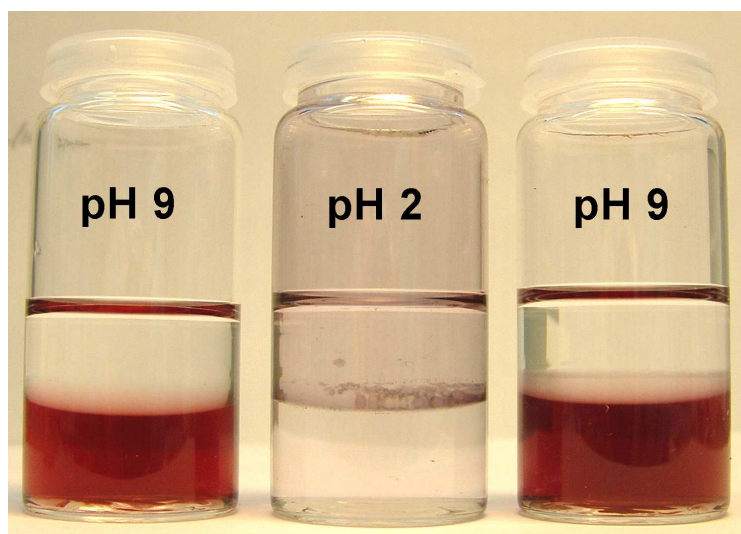


FIGURE S5. Photographs of glass vials containing aqueous solutions (bottom) of 4-MBA capped Au nanoparticles with a mean size of 6 nm in contact with heptane (top). The initial aqueous solution of the nanoparticles in the glass vials was red in colour with pH 9 (left). By adding 1M HCl, the pH of the nanoparticle aqueous solutions was gradually decreased to 2 (middle). After vigorous shaking and storing for 1 h, the thin film of Au nanoparticles, formed at the water/heptane interface, climbed up and coated the interface between heptane and the hydrophilic wall of the glass vial. This film shows a purple transmittance colour. On the right, the pH values of the aqueous solutions were adjusted back to 9 by carefully adding 1M NaOH. The original colour returned the aqueous phase, suggesting the redispersion of the nanoparticles in water.

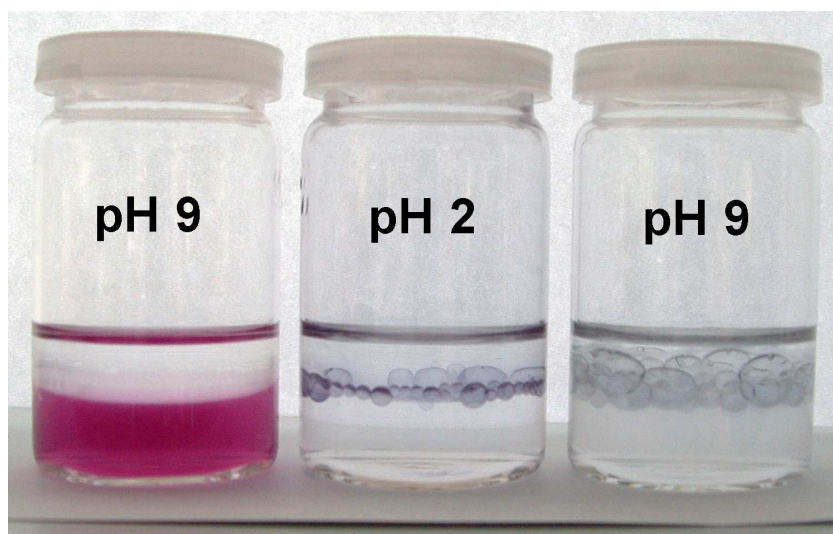


FIGURE S6. Photographs of glass vials containing aqueous solutions (bottom) of 4-MBA capped Au nanoparticles with a mean size of 16 nm in contact with heptane (top). The initial aqueous solution of the nanoparticles in the glass vials was red-purple (b.) in colour with pH 9 (left). By adding 1M HCl, the pH of the nanoparticle aqueous solutions was gradually decreased to 2 (middle). After vigorous shaking and storing for 1 h, the thin film of Au nanoparticles, formed at the water/heptane interface, climbed up and coated the interface between heptane and the hydrophilic wall of the glass vial. This film shows a blue transmittance colour. On the right, the pH values of the aqueous solutions were adjusted back to 9 by carefully adding 1M NaOH. Unlike the 6 nm gold nanoparticles (Figure S5) the thin films of 16 nm nanoparticles remained at the interface.

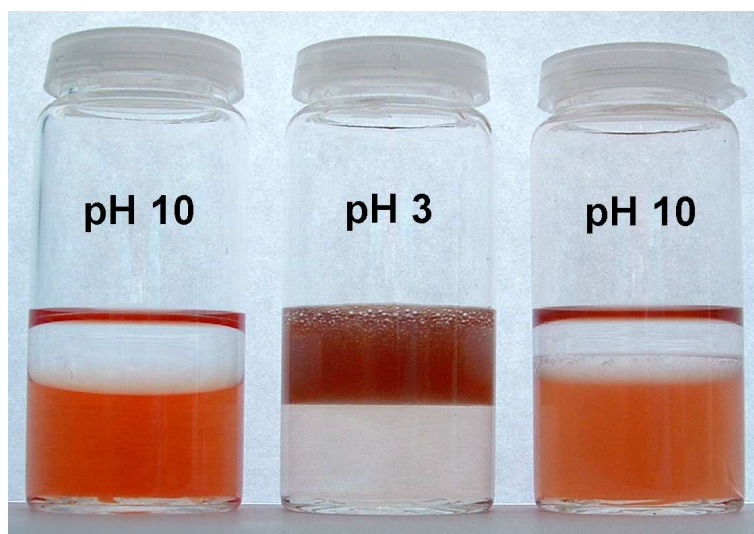


FIGURE S7. Photographs of glass vials containing aqueous solutions (bottom) of 3-MPA capped CdTe nanoparticles with a mean size of 3 nm in contact with heptane (top). The initial aqueous solution of the nanoparticles in the glass vials was orange in colour with pH 10 (left). By adding 1M HCl, the pH of the nanoparticle aqueous solutions was gradually decreased to 3 (middle). After vigorous shaking an unstable emulsion is formed that dissipates over a period of 2 hours. This emulsion has a brown colour indicating the attachment of the CdTe nanoparticles at the water/heptane interface. On the right, the pH values of the aqueous solutions were adjusted back to 10 by carefully adding 1M NaOH. The original colour returned the aqueous phase, suggesting the redispersion of the nanoparticles in water.

REFERENCES

1. H. Reiss, W.K. Kegel, and J. Groenewold. *Ber. Bunsenges. Phys. Chem.*, **100** (1996) 279.
2. F. Reincke, S. G. Hickey, and W. K. Kegel. *Angew. Chem. Int. Ed.*, **43** (2004) 458–462.
3. Hongwei Duan, Dayang Wang, Dirk G. Kurth, and Helmuth Möhwald. *Angewandte Chemie, International Edition*, **43-42** (2004) 5639–5642.
4. R. Aveyard and J. H. Clint. *Journal of the Chemical Society, Faraday Transactions*, **92-1** (1996) 85–89.
5. W.G. Hoover and F.H. Ree. *J.Chem.Phys.*, **49** (1968) 3609–3617.
6. P. Pieranski. *Physical Review Letters*, **45-7** (1980) 569–572.
7. A. J. Hurd. *Journal Of Physics A-Mathematical And General*, **18-16** (1985) 1055–1060.
8. E.J.W. Verwey and J.Th.G. Overbeek. *Theory of stability of lyophobic colloids*. Dover, NY, 1999.

F. Reincke, H. Zhang, M. Nolte, D. Wang, and H. Möhwald: MAX PLANCK INSTITUTE OF COLLOIDS AND INTERFACES, D-14424, POTSDAM, GERMANY, *W.K. Kegel*: VAN'T HOFF LABORATORY FOR PHYSICAL AND COLLOID CHEMISTRY, UTRECHT UNIVERSITY, P.O. BOX 80.000, PRINCETONPLEIN 1, 3508 TA UTRECHT, THE NETHERLANDS, *D. Vanmaekelbergh*: CONDENSED MATTER AND INTERFACES, UTRECHT UNIVERSITY, P.O. BOX 80.000, PRINCETONPLEIN 1, 3508 TA UTRECHT, THE NETHERLANDS

E-mail address: `dayang.wang@mpikg-golm.mpg.de`